Monthly Notices
of the
ROYAL ASTRONOMICAL SOCIETY

MNRAS **510,** 4808–4818 (2022) https://doi.org/10.1093/mnras/stab3759
Advance Access publication 2021 December 29

Radiative lifetimes, branching fractions, and oscillator strengths for highly excited levels in singly ionized tantalum (Ta II)

Lijun Zhang,[1] Yaxin Wu,[1] Meina Liu,[1] Huiting Ma,[1] Pascal Quinet[2,3]★ and Zhenwen Dai[1]★
[1]College of Physics, Jilin University, Changchun 130012, China
[2]Physique Atomique et Astrophysique, Université de Mons, B-7000 Mons, Belgium
[3]IPNAS, Université de Liège, B-4000 Liège, Belgium

Accepted 2021 December 20. Received 2021 December 11; in original form 2021 September 26

ABSTRACT

Radiative lifetimes of 28 levels of Ta II in the energy range 29256.907–55128.389 cm^{-1} were measured by time-resolved laser-induced fluorescence (TR-LIF) spectroscopy in laser-ablation plasma. Among the results, to our knowledge, 24 lifetimes are reported for the first time. These lifetimes, ranging from 2.7 to 111 ns, were combined with theoretical branching fractions obtained from pseudo-relativistic Hartree–Fock calculations including core-polarization effects to deduce semi-empirical transition probabilities and oscillator strengths for 284 Ta II spectral lines.

Key words: atomic data – methods: laboratory: atomic – techniques: spectroscopic.

1 INTRODUCTION

Accurate radiative parameters of heavy-element ions have important applications in the fields of astrophysics and plasma physics. In astrophysics, investigations of the chemical composition of astrophysical objects by simulations of their spectra hinge critically on reliable and sufficient atomic radiative data. In the last two decades, a number of Ta II lines have been observed in the spectra of some stars: the chemically peculiar star χ Lupi (Eriksson et al. 2002), the uranium-rich metal-poor star CS 31082–001 (Siqueira et al. 2013), and the hot Am star HR 3383 (Wahlgren, Nielsen & Leckrone 2021), and the Ta abundances or its upper limits for these stars were estimated. So far, however, the solar photospheric abundance of Ta has not yet been determined (Asplund et al. 2021), and the Ta abundance in our solar system was inferred from meteoritic analysis (Anders & Grevesse 1989). It is basically certain that tantalum is one of the least abundant elements in the solar system and even in most of other celestial bodies. This situation and the problem of inadequate radiative parameters lead to difficulties in Ta abundance studies (Wahlgren et al. 2021). The complexity of Ta II spectra severely limits the determination of experimental transition probabilities (gA) because reliable branching fractions (BFs) are needed for combination with radiative lifetimes (Quinet et al. 2009).

Some researches have been done previously on the radiative parameters of Ta II. Kwiatkowski et al. (1984) first reported the natural radiative lifetimes of six Ta II levels by selective laser excitation and time-resolved observation. Bergström et al. (1986) and Schade & Helbig (1986) used the same method to measure the lifetimes of eight and 10 levels, respectively. Langhans, Schade & Helbig (1995) used tunable picosecond laser pulses for selective excitations to measure 15 short-lived energy levels. Henderson et al. (1999) used the beam-foil method to measure the lifetimes of six Ta II levels, and determined the oscillator strengths of five transitions by combining these lifetimes with the branching fractions deduced from the gA values reported by Corliss & Bozman (1962). Quinet et al. (2009) measured the lifetimes of three odd-parity levels by the time-resolved laser-induced fluorescence (TR-LIF) method and calculated the BFs and transition probabilities for transitions originating from 14 odd-parity levels by the relativistic Hartree–Fock method.

According to the NIST atomic data base (Kramida et al. 2021), which is based on Ta II energy levels from Moore (1958) and the data published by Kiess (1962), Wyart et al. (1977, 1990), Windholz, Arcimowicz & Uddin (2016), and Stachowska et al. (2017), 296 energy levels are currently experimentally established in this ion. To our knowledge, the radiative lifetimes were measured for 34 energy levels in the region of 33 706 to 49 888 cm^{-1}, and the experimental gA and gf (oscillator strength) of 272 spectral lines and the semi-empirical gA of 100 lines were reported. However, the radiative parameters of most of the levels in Ta II are still unknown, especially for the highly excited levels. Therefore, in this work, we expand the radiative parameter measurements for Ta II levels and obtain the radiative lifetimes of 28 levels of Ta II in the region of 29 256.907–55 128.389 cm^{-1} by the TR-LIF technique. By combining these lifetimes with theoretical BFs calculated using the pseudo-relativistic Hartree–Fock method, including core-polarization corrections, a new set of gA and gf-values was deduced for 284 Ta II spectral lines. These data will greatly enrich the radiative data of Ta II and be very helpful for the analysis of astronomical spectra.

2 LIFETIME MEASUREMENTS

The experimental method used to measure the lifetime of TR-LIF in this paper is the same as the previous method used by our group (Tian et al. 2016), so here we give only a brief description. In the experiment, we employed a single-step excitation scheme. A 532 nm Q-switched Nd: YAG laser with 8 ns pulse duration, 10 Hz repetition rate, and pulse energy of 5–10 mJ was used as an ablation beam to

---

★ E-mail: pascal.quinet@umons.ac.be (PQ); dai@jlu.edu.cn (ZD)

Published by Oxford University Press on behalf of Royal Astronomical Society

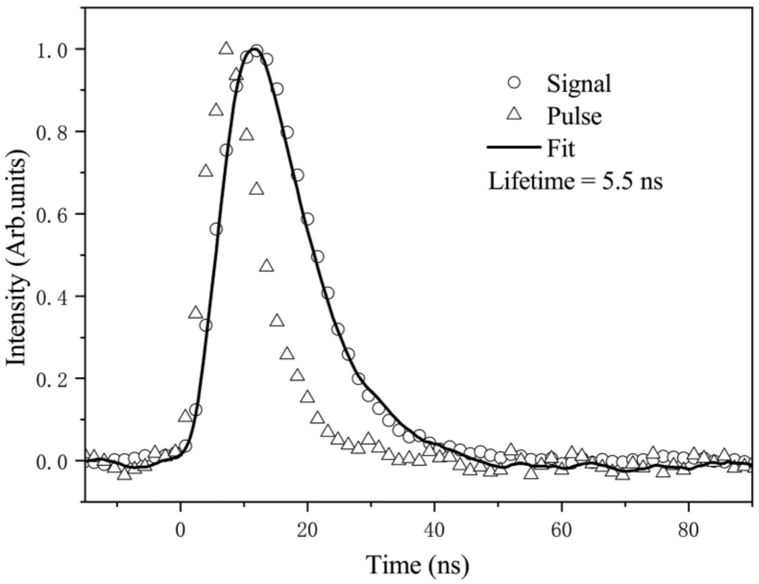

Figure 1. A typical fluorescence decay curve of the Ta II level 44430.422 cm^{-1} with the fitted convolution curve between the laser pulse and an exponential.

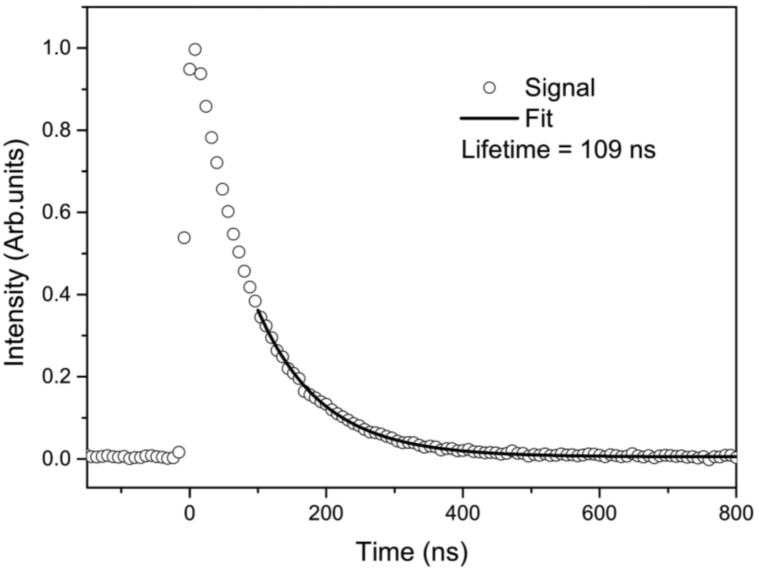

Figure 2. A typical fluorescence decay curve of the Ta II level 36113.091 cm^{-1} with an exponential fit.

generate laser plasma of Ta. A dye laser using 4-dicyanomethylene-2-methyl-6-(p-dimethylaminostyryl)-4H-pyran (DCM) and Rhodamine 6 G dyes, which was pumped by another Nd: YAG laser with the same performance parameters as the former except for pulse energy, produced a tunable laser in the 604–658 and 558–588 nm regions, respectively. To further expand the laser wavelength, one or two β-barium borate (BBO) crystals were used to generate the second or the third harmonic light of the dye laser. Excitation pulses with a duration of about 6 ns were horizontally fed into a vacuum chamber to excite Ta ions. Fluorescence of excited ions is collected with a grating monochromator, and then detected by a photomultiplier tube (Hamamatsu R3896) and recorded by a digital oscilloscope (Tektronix TDS 620B).

In the experiment, we used a high-precision wavemeter (High-Finesse WS6) to monitor the dye laser wavelength for avoiding false excitation to other levels. In order to wash away the quantum beats generated by the Earth's magnetic field and to reduce the recombination background in the plasma, a magnetic field of about 100 G was applied to the plasma by a pair of Helmholtz coils (Wang et al. 2018). In the experiment, several systematic effects, including the saturation, collision, radiation trapping, and flight-out-of-view effects, may influence lifetime measurements. All of them were minimized by optimizing experimental conditions as described by Wang et al. (2018).

In the measurement, to obtain a good signal-to-noise ratio, each fluorescence decay curve was averaged over 1000 times. For each level, more than 10 curves were recorded under different conditions. The average of the lifetime values assessed by these curves was taken as the final lifetime. For the lifetime value shorter than five times the duration of excitation pulse, it must be evaluated by fitting the fluorescence decay curve to the convolution of the detected laser pulse and a purely exponential function. A typical fluorescence decay

Table 1. Configurations explicitly included in the atomic structure calculations for Ta II.

HFR + CPOL(A) Even parity	Odd parity	HFR + CPOL(B) Even parity	Odd parity
$5d^36s$	$5d^36p$	$5d^36s$	$5d^36p$
$5d^37s$	$5d^37p$	$5d^37s$	$5d^37p$
$5d^36d$	$5d^35f$	$5d^36d$	$5d^35f$
$5d^4$	$5d^36f$	$5d^4$	$5d^36f$
$5d^26s^2$	$5d^26s6p$	$5d^26s^2$	$5d^26s6p$
$5d^26p^2$	$5d^26s7p$	$5d^26p^2$	$5d^26s7p$
$5d^26d^2$	$5d^26s5f$	$5d^26d^2$	$5d^26s5f$
$5d^27s^2$	$5d^26s6f$	$5d^27s^2$	$5d^26s6f$
$5d^26s6d$	$5d^26p6d$	$5d^26s6d$	$5d^26p6d$
$5d^26s7s$	$5d^26p7s$	$5d^26s7s$	$5d^26p7s$
$5d^26p5f$	$5d6s^26p$	$5d^26p5f$	$5d6s^26p$
$5d^26d7s$	$5d6s^25f$	$5d^26d7s$	
$5d6s^26d$	$5d6s^26f$		
$5d6s^27s$	$5d6p^3$		
$5d6s6p^2$	$5d6s6p6d$		
$5d6s6p5f$	$5d6s6p7s$		
$5d6s7s^2$	$6s6p^3$		
$6s26p^2$	$6s^26p7s$		
$6s^26p5f$	$6s^26p6d$		

curve for the 44 430.422 $\mathrm{cm^{-1}}$ level with a 5.5 ns lifetime is shown in Fig. 1. For other longer lifetimes, the decay curves were fitted by least-squares exponentials. This fitting process must choose an appropriate starting point to avoid the influence of excitation pulse (Shang et al. 2015). A typical fluorescence decay curve for the 36 113.091 $\mathrm{cm^{-1}}$ level with a 109 ns lifetime is shown in Fig. 2. As seen in Figs 1 and 2, the fitted curves are in good agreement with the measured fluorescence curves.

3 RADIATIVE PARAMETER CALCULATIONS

In addition to the experimental measurements, we also performed calculations of lifetimes, branching fractions, transition probabilities and oscillator strengths in this work, in order to produce a set of radiative parameters as reliable as possible for Ta II lines, usable for the analysis of spectra observed from astrophysical or laboratory plasmas. These were done using the relativistic Hartree–Fock method, originally introduced by Cowan (1981), in which core-polarization effects were added, resulting in the HFR + CPOL method, as described e.g. by Quinet et al. (1999, 2002) and Quinet (2017). The starting point for these calculations was to use the same two physical models, HFR + CPOL(A) and HFR + CPOL(B), as those previously considered by Quinet et al. (2009). These models differ essentially in the way intravalence interactions and core polarization corrections are taken into account. As a reminder, in the first model [HFR + CPOL(A)], a Ta VI ionic core surrounded by four valence electrons was considered, while, in the HFR + CPOL(B) model, a Ta IV core surrounded by two valence electrons was retained. This gave rise to the explicit inclusion in the calculations of the configurations listed in Table 1 and core-polarization parameters given by $\alpha_d = 3.18$ au, $r_c = 1.30$ au [HFR + CPOL(A)] and $\alpha_d = 6.75$ au, $r_c = 1.95$ au [HFR + CPOL(B)], where α_d represents the dipole polarizability of the ionic core taken from Fraga et al. (1976) and r_c is the cut-off radius corresponding to the HFR mean value of r for the outermost core orbitals, i.e. $<r>_{5p}$ in the case of CPOL(A) and $<r>_{5d}$ in the case of CPOL(B). A slight difference with the work carried out by Quinet et al. (2009) is that, since this latter study, the experimental Ta II levels have been revised by Windholz et al. (2016), allowing for a refinement of the semi-empirical adjustment of the radial parameters from Quinet et al's fit that had been performed using the energy levels established by Kiess (1962), Wyart (1977) and Wyart and Blaise (1990). However, due to the small differences between the new and the old experimental level values, no drastic changes were observed in the fitting process, the standard deviations being found to be the same as those obtained by Quinet et al. (2009), i.e. 60 and 120 $\mathrm{cm^{-1}}$ [HFR + CPOL(A)] and 60 and 140 $\mathrm{cm^{-1}}$ [HFR + CPOL(B)], for the even and odd parities, respectively.

4 RESULTS AND DISCUSSION

In this paper, the radiative lifetimes of 28 levels of Ta II in the energy range of 29 256.907–55 128.389 $\mathrm{cm^{-1}}$ were determined as listed in Table 2 with quoted error bars, which consist of possible remaining systematic errors and statistical scattering errors from different recordings. Among them, four levels were also studied in literature by experiments and/or calculations for which their previous results are also presented for comparison. For the 36 763.763, 41 775.294, and 44 430.422 $\mathrm{cm^{-1}}$ levels, our experimental results are in rather good agreement with those measured by Kwiatkowski et al. (1984), Schade & Helbig (1986), Henderson et al. (1999), and Langhans et al. (1995). But for the 38962.377 $\mathrm{cm^{-1}}$ level, the result presented by Schade & Helbig (1986) is 6.2(4) ns, which has a slightly larger difference than our value of 5.4(3) ns. Schade & Helbig (1986) measured lifetimes of 10 levels, for which six lifetimes were also presented by Kwiatkowski et al. (1984) for five levels, Bergström et al. (1986) for four levels, and Henderson et al. (1999) for one level. It is seen that all the values by Schade & Helbig (1986) are larger than the results in other papers. Moreover, the same is true for the three levels measured in this work and by Schade & Helbig (1986). Therefore, we may conclude that our result for the 38 962.377 $\mathrm{cm^{-1}}$ level may be more reliable.

To our best knowledge, the lifetimes of 24 levels out of the 28 Ta II levels measured in this work are reported for the first time. The measured lifetime values are in the range between 2.7 and 111 ns, and their uncertainties are smaller than 10 per cent, except for two levels, 48 233.051 and 48 776.276 $\mathrm{cm^{-1}}$, with somewhat larger uncertainties of 10.4 and 11.5 per cent, respectively.

In Table 2, we also give the calculated lifetimes obtained using our HFR + CPOL(A) and HFR + CPOL(B) theoretical models. It is interesting to note that Quinet et al. (2009) stated that, on the basis of comparisons between their theoretical results and available experimental lifetimes, it was not obvious to decide which of the latter two models provided the best description of the data. Indeed, for two of the three levels measured by Quinet et al., the HFR + CPOL(B) model appeared to be in better agreement with the experimental results than the HFR + CPOL(A) model, while the opposite was true for the third level. In addition, the model A was found to be in good agreement with the experimental results of both Kwiatkowski et al. (1984) and Bergström et al. (1986), while, on the other hand, the model B showed a better agreement with the experimental lifetimes of Schade & Helbig (1986). The rather large number of new accurate lifetimes measured in this work provides an attractive opportunity to test once again the two theoretical models considered. When doing such a comparison, we note that model B shows slightly better overall agreement with our new experimental lifetimes than model A. Indeed, the average ratios $\tau_{\mathrm{HFR+CPOL(B)}}/\tau_{\mathrm{exp}} = 0.98 \pm 0.26$ and $\tau_{\mathrm{HFR+CPOL(A)}}/\tau_{\mathrm{exp}} = 0.86 \pm 0.22$, where the uncertainty represents the standard deviation of the mean, show that our HFR + CPOL(A)

Table 2. Measured and calculated lifetimes of Ta II levels and their comparison with previous results.

Upper level[a]		Lower level[a]		$\lambda_{\mathrm{Exc.}}$ (nm)[b]	$\lambda_{\mathrm{Obs.}}$ (nm)[b]	Lifetime (ns)					
Assignment	E (cm^{-1})	J	E (cm^{-1})			This work			Previous		
						Exp.	HFR(A)	HFR(B)	Exp.	HFR(A)[c]	HFR(B)[c]
292°_2	29 256.907	2	13 560.293	637.080	375	111(9)	115.9	126.6			
361°_3	36 113.091	4	4415.750	315.485	328	109(10)	90.7	122.1			
367°_3	36 763.763	4	4415.750	309.138	321	15.4(3)	16.7	21.2	15.8(9)[d], 15.4(9)[e]	16.7	21.2
$^5\mathrm{G}^\circ_3$	38 962.377	3	6831.437	311.226	263	5.4(3)	3.6	4.5	6.2(4)[d]	3.6	4.5
400°_0	40 023.635	1	5330.822	288.242	249	11.3(2)	10.4	13.6			
402°_2	40 233.533	1	5330.822	286.509	286	26.6(18)	11.6	19.3			
403°_1	40 304.766	2	5657.920	288.627	248	7.6(5)	7.0	8.7			
413°_1	41 355.040	2	9690.482	315.810	261	11.0(1)	9.3	13.0			
415°_3	41 554.386	2	9690.482	313.833	260	9.7(4)	11.0	13.2			
417°_5	41 708.994	4	9746.376	312.865	268	16.4(6)	15.7	17.2			
417°_4	41 775.294	4	9746.376	312.217	371	6.4(3)	4.9	6.7	6.2(6)[f], 6.6(5)[d]	4.9	6.7
$^5\mathrm{F}^\circ_4$	42 122.941	3	6831.437	283.354	308	7.4(4)	7.0	8.1			
421°_2	42 153.276	3	6831.437	283.110	243	9.2(8)	10.5	12.3			
444°_3	44 430.422	2	9690.482	287.853	249	5.5(5)	4.3	5.9	6.0(3)[g]		
482°_2	48 223.051	2	1031.416	211.901	207	4.8(5)	3.1	3.8			
486°_2	48 666.557	2	1031.416	209.929	209	6.1(4)	5.4	5.7			
487°_1	48 776.276	2	1031.416	209.446	205	8.7(10)	2.7	3.4			
489°_3	48 962.626	2	1031.416	208.632	208	10.3(5)	8.3	9.0			
495°_2	49 592.90	3	2642.302	212.989	212	7.8(3)	3.7	3.5			
503°_3	50 314.638	3	2642.302	209.765	209	4.8(2)	3.3	3.7			
521°_1	52 155.811	0	4124.858	208.199	204	2.7(2)	2.2	3.1			
525°_3	52 580.519	4	4415.750	207.621	200	2.8(2)	1.7	2.0			
528°_1	52 824.611	1	5330.822	210.553	212	3.1(3)	2.4	2.9			
534°_3	53 465.73	2	5657.920	209.171	196	3.0(3)	2.7	3.4			
536°_2	53 644.90	1	5330.822	206.979	196	2.8(2)	2.1	2.9			
545°_2	54 533.758	3	6831.437	209.633	186	4.4(2)	3.9	3.1			
546°_3	54 648.975	3	6831.437	209.129	192	3.2(2)	2.4	2.1			
551°_3	55 128.389	3	6831.437	202.141	202	3.2(2)	2.1	2.8			

[a] Assignments and J values are from Kramida et al. (2021) except that the one of the 50 314.638 cm^{-1} level is from Kiess (1962), and energy values are from Windholz et al. (2016).
[b] The wavelengths are the vacuum values.
[c] Quinet et al. (2009).
[d] Schade & Helbig (1986).
[e] Kwiatkowski et al. (1984).
[f] Henderson et al. (1999).
[g] Langhans et al. (1995).

lifetimes are globally systematically shorter than the experimental values, which is not the case with the HFR + CPOL(B) results.

In Table 3, we list the transitions depopulating the levels for which we measured the radiative lifetimes in our work. For each of these transitions, we give the BFs calculated with the HFR + CPOL(A) and HFR + CPOL(B) methods, limiting ourselves to BFs > 0.01. For each upper level, we also give the residuals of branching fractions between brackets. In the large majority of cases, these residuals are of a few per cent. However, more important residuals appear for some levels, such as those at 54 648.975 and 55 128.389 cm^{-1} for example. These are due to the very large number of very weak transitions (with BF < 0.01) depopulating these levels and whose line strengths are also affected by strong cancellation effects, which explains why the residuals obtained with HFR + CPOL(A) and HFR + CPOL(B), and thus the whole set of BF-values, are in less good agreement for these particular levels.

These BF-values, combined with the experimental lifetimes, were used to determine the gA and log gf, also included in Table 3. As already noticed by Quinet et al. (2009) for a smaller sample of Ta II lines, the BFs obtained in our two calculations agree quite well with each other (generally within a few per cent particularly for the transitions with BF-values larger than 0.10). This implies that the gA- and gf-values obtained using the combination of the experimental lifetimes with both the HFR + CPOL(A) and HFR + CPOL(B) BFs agree quite well for the most intense transitions so that the use of either set of results for different applications in astrophysical or laboratory plasmas is roughly the same. However, as shown in Fig. 3, where both sets of log gf-values are compared with each other, larger discrepancies can be observed for some data. More precisely, it was found that a handful (12 per cent) of transitions considered in this work gave discrepancies larger than 0.3 dex (which corresponds to a factor of two in the gf-values). These discrepancies are, of course, due to the differences between the BF-values obtained from the HFR + CPOL(A) and HFR + CPOL(B) models for specific levels such as those at 48 666.557, 54 648.975, and 55 128.389 cm^{-1} for which our calculations showed very strong mixings in the eigenvector compositions as well as large cancellation effects in the line strengths for transitions depopulating them. If a preference should be given, in view of the better overall agreement between the experimental lifetimes and the values obtained with the HFR + CPOL(B) model,

Table 3. Branching fractions, transition probabilities, and oscillator strengths obtained in this work of Ta II levels and their comparison with previous results.

Upper level[a]		Lower level[a]		λ (nm)[b]	BF[c]		*gA* (10^6 s^{-1})			log(*gf*)		
Assignment	*E* (cm^{-1}) Lifetime (ns)	Assignment	*E* (cm^{-1})		HFR (A)	HFR (B)	This work HFR (A)	This work HFR (B)	Previous	This work HFR (A)	This work HFR (B)	Previous
292°_2	29 256.907	5d^3(^{4}F)6s a^{5}F$_2$	1031.416	354.189	0.099	0.107	4.48	4.83	38.0[f]	−2.07	−2.04	−1.14[f]
	$\tau = 111(9)$	5d^{2}6s^2 a^{3}F$_2$	3180.141	383.374	0.747	0.721	33.7	32.5	70.0[f]	−1.13	−1.14	−0.81[f]
		5d^3(^{4}F)6 s b^{3}F$_2$	9690.482	510.938	0.073	0.072	3.29	3.23	8.50[f]	−1.89	−1.90	−1.48[f]
		5d^3(^{4}P)6 s a^{5}P$_2$	11 875.525	575.168	0.025	0.023	1.11	1.04		−2.26	−2.29	
		5d^3(^{2}D2)6 s a^{3}D$_1$	14 627.680	683.374	0.011	0.012	0.47	0.56		−2.48	−2.41	
					[0.045]	[0.065]						
361°_3	36 113.091	5d^3(^{4}F)6s a^{5}F$_3$	2642.302	298.681	0.352	0.253	29.0	20.9	240[f]	−1.41	−1.55	−0.49[f]
	$\tau = 109(10)$	5d^3(^{4}F)6s a^{5}F$_4$	4415.750	315.393	0.051	0.051	4.25	4.19		−2.20	−2.20	
		5d^{2}6s^2 a^{3}F$_3$	6831.437	341.413	0.491	0.569	40.5	47.0	360[f]	−1.15	−1.09	−0.21[f]
		5d^{2}6s^2 a^{3}F$_4$	9746.376	379.158	0.032	0.044	2.67	3.67		−2.24	−2.10	
		5d^3(^{2} G)6s a^{3}G$_4$	12 705.388	427.090	0.034	0.040	2.81	3.32		−2.11	−2.04	
		5d^3(^{2}H)6s a^{3}H$_4$	15 851.163	493.398	0.016	0.019	1.3	1.55		−2.32	−2.25	
					[0.024]	[0.024]						
367°_3	36 763.763	5d^3(^{4}F)6s a^{5}F$_2$	1031.416	279.776	0.603	0.615	274	279	271[d],	−0.49	−0.48	
	$\tau = 15.4(3)$								1600[f]			0.26[f]
		5d^{2}6s^2 a^{3}F$_2$	3180.141	297.677	0.058	0.048	26.2	21.9	25.8[d]	−1.46	−1.54	
		5d^{2}6s^2 a^{3}P$_2$	5657.920	321.390	0.123	0.114	56.0	51.8	55.3[d],	−1.06	−1.10	
									580[f]			−0.05[f]
		5d^{2}6s^2 a^{3}F$_3$	6831.437	333.991	0.112	0.118	50.8	53.4	50.2[d],	−1.07	−1.05	
									390[f]			−0.18[f]
		5d^{2}6s^2 a^{3}F$_4$	9746.376	370.027	0.015	0.019	6.85	8.42	6.78[d]	−1.85	−1.76	
		5d^4 a^{5}D$_2$	14 494.870	448.931	0.011	0.013	4.99	5.84	4.94[d]	−1.82	−1.75	
					[0.078]	[0.073]						
$^5G^{\circ}_3$	38 962.377	5d^3(^{4}F)6s a^{5}F$_2$	1031.416	263.558	0.587	0.578	761	749	663[d],	−0.10	−0.11	
	$\tau = 5.4(3)$								4800[f]			0.70[f]
		5d^3(^{4}F)6s a^{5}F$_3$	2642.302	275.249	0.366	0.378	474	490	413[d],	−0.27	−0.25	
									1700[f]			0.29[f]
		5d^3(^{4}F)6s b^{3}F$_2$	9690.482	341.527	0.018	0.017	23.8	21.9	20.7[d]	−1.38	−1.42	
					[0.029]	[0.027]						
400°_0	40 023.635	5d^3(^{4}F)6s a^{5}F$_1$	0.000	249.777	0.125	0.050	11.1	4.41	220[f]	−1.98	−2.38	0.69[f]
	$\tau = 11.3(2)$	5d^{2}6s^2 a^{3}P$_1$	5330.822	288.159	0.722	0.768	63.9	67.9		−1.10	−1.07	
		5d^3(^{4}P)6s a^{5}P$_1$	10 713.345	341.079	0.022	0.022	1.97	1.94		−2.46	−2.47	
		5d^4 a^{5}D$_1$	13 475.416	376.566	0.091	0.105	8.09	9.28		−1.76	−1.70	
		5d^3(^{2}D2)6s a^{3}D$_1$	14 627.680	393.652	0.012	0.021	1.09	1.82		−2.60	−2.37	
		5d^3(^{4}P)6s b^{3}P$_1$	17 375.124	441.406	0.022	0.027	1.95	2.41		−2.24	−2.15	
					[0.006]	[0.007]						
402°_2	40 233.533	5d^3(^{4}F)6s a^{5}F$_1$	0.000	248.474	0.063	0.121	11.8	22.8	370[f]	−1.96	−1.68	−0.47[f]
	$\tau = 26.6(18)$	5d^3(^{4}F)6s a^{5}F$_2$	1031.416	255.011	0.097	0.086	18.2	16.2		−1.75	−1.80	
		5d^3(^{4}F)6s a^{5}F$_3$	2642.302	265.941	0.387	0.287	72.7	53.9	490[f]	−1.11	−1.24	−0.28[f]
		5d^{2}6s^2 a^{3}F$_2$	3180.141	269.801	0.029	0.033	5.37	6.29		−2.23	−2.16	
		5d^{2}6s^2 a^{3}P$_1$	5330.822	286.427	0.121	0.082	22.7	15.5		−1.55	−1.72	
		5d^{2}6s^2 a^{3}P$_2$	5657.920	289.136	0.148	0.149	27.7	28.0		−1.46	−1.45	
		5d^{2}6s^2 a^{3}F$_3$	6831.437	299.295	0.065	0.084	12.3	15.7		−1.78	−1.68	
		5d^3(^{4}F)6s b^{3}F$_2$	9690.482	327.313	0.029	0.041	5.38	7.70		−2.06	−1.91	
		5d^4 a^{5}D$_1$	13 475.416	373.612	0.011	0.026	2.10	4.84		−2.36	−1.99	
		5d^{2}6s^2 a^{1}D$_2$	13 560.293	374.801	0.012	0.028	2.21	5.17		−2.33	−1.96	
					[0.038]	[0.063]						
403°_1	40 304.766	5d^3(^{4}F)6s a^{5}F$_1$	0.000	248.035	0.012	0.034	4.62	13.5		−2.37	−1.90	
	$\tau = 7.6(5)$	5d^3(^{4}F)6s a^{5}F$_2$	1031.416	254.550	0.290	0.230	115	90.9	1200[f]	−0.95	−1.05	0.05[f]
		5d^{2}6s^2 a^{3}F$_2$	3180.141	269.283	0.057	0.061	22.5	24.3	250[f]	−1.61	−1.58	−0.56[f]
		5d^{2}6s^2 a^{3}P$_1$	5330.822	285.843	0.412	0.426	163	168	1400[f]	−0.70	−0.69	0.23[f]
		5d^{2}6s^2 a^{3}P$_2$	5657.920	288.542	0.088	0.074	34.7	29.1	540[f]	−1.36	−1.44	−0.17[f]
		5d^3(^{4}F)6s b^{3}F$_2$	9690.482	326.551	0.061	0.078	23.9	30.7		−1.42	−1.31	
		5d^4 a^{5}D$_0$	12 600.801	360.856	0.011	0.014	4.34	5.39		−2.07	−1.98	
		5d^4 a^{5}D$_1$	13 475.416	372.620	0.012	0.012	4.61	4.57		−2.02	−2.02	
		5d^4 a^{5}D$_2$	14 494.870	387.338	0.022	0.022	8.55	8.76		−1.72	−1.71	
					[0.035]	[0.049]						
413°_1	41 355.040	5d^3(^{4}F)6s a^{5}F$_1$	0.000	241.735	0.086	0.078	23.3	21.4	310[f]	−1.69	−1.73	−0.57[f]

Table 3 – *continued*

Upper level[a]	E (cm^{-1})	Lower level[a]		λ (nm)[b]	BF[c]		gA (10^6 s^{-1})			log(gf)		
Assignment	Lifetime (ns)	Assignment	E (cm^{-1})		HFR (A)	HFR (B)	This work HFR (A)	This work HFR (B)	Previous	This work HFR (A)	This work HFR (B)	Previous
	$\tau = 11.0(1)$	$5d^26s^2\ a^3P_0$	4124.858	268.519	0.232	0.235	63.2	64.0	12 300^f	−1.16	−1.16	1.12^f
		$5d^26s^2\ a^3P_1$	5330.822	277.509	0.359	0.325	98.0	88.7	1100^f	−0.95	−0.99	0.09^f
		$5d^26s^2\ a^3P_2$	5657.920	280.052	0.015	0.010	3.99	2.62		−2.33	−2.51	
		$5d^3(^4F)6s\ b^3F_2$	9690.482	315.720	0.032	0.041	8.68	11.1		−1.89	−1.78	
		$5d^3(^4P)6s\ a^5P_1$	10 713.345	326.259	0.077	0.086	21.1	23.4		−1.47	−1.43	
		$5d^3(^4P)6s\ a^5P_2$	11 875.525	339.122	0.015	0.022	4.01	6.11		−2.16	−1.98	
		$5d^4\ a^5D_1$	13 475.416	358.583	0.021	0.023	5.70	6.41		−1.96	−1.91	
		$5d^4\ a^5D_2$	14 494.870	372.192	0.043	0.054	11.8	14.8		−1.61	−1.51	
		$5d^3(^4P)6s\ b^3P_2$	18 500.717	437.431	0.059	0.062	16.0	16.9		−1.34	−1.32	
					[0.061]	[0.064]						
415°_3	41 554.386	$5d^3(^4F)6s\ a^5F_2$	1031.416	246.699	0.082	0.076	59.2	54.6	860^f	−1.27	−1.30	−0.11^f
	$\tau = 9.7(4)$	$5d^3(^4F)6s\ a^5F_3$	2642.302	256.913	0.114	0.098	82.4	70.8	2200^f	−1.09	−1.15	0.35^f
		$5d^3(^4F)6s\ a^5F_4$	4415.750	269.181	0.013	0.034	9.21	24.3	430^f	−2.00	−1.58	−0.33^f
		$5d^26s^2\ a^3P_2$	5657.920	278.497	0.161	0.172	116	124	1300^f	−0.87	−0.84	0.19^f
		$5d^26s^2\ a^3F_3$	6831.437	287.910	0.081	0.074	58.5	53.7	620^f	−1.14	−1.18	−0.11^f
		$5d^3(^4F)6s\ b^3F_2$	9690.482	313.744	0.086	0.075	62.1	53.9	670^f	−1.04	−1.10	−0.00^f
		$5d^26s^2\ a^3F_4$	9746.376	314.295	0.120	0.107	86.5	77.2	670^f	−0.89	−0.94	−0.00^f
		$5d^3(^4P)6s\ a^5P_2$	11 875.525	336.843	0.063	0.073	45.3	53.0		−1.11	−1.04	
		$5d^3(^4P)6s\ a^5P_3$	12 435.879	343.326	0.021	0.022	15.3	15.7		−1.57	−1.56	
		$5d^3(^2G)6s\ a^3G_4$	12 705.388	346.533	0.035	0.039	25.4	27.9		−1.34	−1.30	
		$5d^3(^2G)6S\ ^3G_4$	12 966.096	349.694	0.010	0.011	7.47	7.64		−1.86	−1.85	
		$5d^26s^2\ a^1D_2$	13 560.293	357.116	0.017	0.012	12.1	8.44		−1.64	−1.79	
		$5d^4\ a^5D_2$	14 494.870	369.451	0.077	0.074	55.7	53.8	690^f	−0.94	−0.96	0.15^f
		$5d^4\ a^5D_3$	15 726.100	387.062	0.042	0.044	304	32.1		−1.16	−1.14	
		$5d^3(^2H)6s\ a^3H_4$	15 851.163	388.946	0.029	0.034	20.7	24.5		−1.33	−1.25	
					[0.049]	[0.055]						
417°_5	41 708.994	$5d^3(^4F)6s\ a^5F_4$	4415.750	268.065	0.330	0.337	221	226	2000^f	−0.62	−0.61	0.32^f
	$\tau = 16.4(6)$	$5d^3(^4F)6s\ a^5F_5$	6186.780	281.431	0.102	0.146	68.7	97.7	950^f	−1.09	−0.94	0.05^f
		$5d^26s^2\ a^3F_4$	9746.376	312.774	0.305	0.290	204	194	1800^f	−0.52	−0.54	0.41^f
		$5d^3(^2G)6s\ a^3G_4$	12 705.388	344.686	0.126	0.104	84.6	69.9	970^f	−0.82	−0.90	0.24^f
		$5d^3(^2H)6s\ ^3G_5$	14 158.542	362.867	0.043	0.042	29.0	28.4		−1.24	−1.25	
		$5d^3(^2H)6s\ a^3H_4$	15 851.163	386.620	0.081	0.070	54.4	47.2		−0.91	−0.98	
					[0.013]	[0.011]						
417°_4	41 775.294	$5d^3(^4F)6s\ a^5F_3$	2642.302	255.462	0.345	0.349	485	490	485^d	−0.32	−0.32	
	$\tau = 6.4(3)$	$5d^3(^4F)6s\ a^5F_4$	4415.750	267.589	0.512	0.481	721	676	721^d	−0.11	−0.14	0^e
		$5d^26s^2\ a^3F_3$	6831.437	286.089	0.044	0.051	62.5	71.2	62.5^d	−1.11	−1.06	
		$5d^26s^2\ a^3F_4$	9746.376	312.128	0.010	0.021	14.7	29.1	14.6^d	−1.67	−1.37	
		$5d^3(^2G)6s\ a^3G_3$	11 767.242	333.148	0.013	0.012	18.4	16.3	18.4^d	−1.51	−1.57	
		$5d^3(^4P)6s\ a^5P_3$	12 435.879	340.740	0.030	0.030	42.4	42.4	39.6^d	−1.13	−1.13	
		$5d^3(^2G)6s\ a^3G_4$	12 705.388	343.899	0.022	0.030	30.4	41.9	30.4^d	−1.27	−1.13	
					[0.024]	[0.026]						
$^5F^\circ_4$	42 122.941	$5d^3(^4F)6s\ a^5F_3$	2642.302	253.213	0.477	0.525	580	638	4800^f	−0.25	−0.21	0.66^f
	$\tau = 7.4(4)$	$5d^3(^4F)6s\ a^5F_4$	4415.750	265.122	0.246	0.233	300	284	2700^f	−0.50	−0.52	0.45^f
		$5d^26s^2\ a^3F_3$	6831.437	283.271	0.044	0.047	53.7	57.7	710^f	−1.19	−1.16	−0.07^f
		$5d^26s^2\ a^3F_4$	9746.376	308.775	0.084	0.077	102	93.7	780^f	−0.84	−0.87	0.05^f
		$5d^3(^2G)6s\ a^3G_3$	11 767.242	329.332	0.014	0.010	17.1	12.4		−1.56	−1.69	
		$5d^3(^4P)6s\ a^5P_3$	12 435.879	336.750	0.017	0.011	21.0	13.3		−1.45	−1.65	
		$5d^3(^2G)6s\ a^3G_4$	12 705.388	339.835	0.046	0.041	56.3	49.7		−1.01	−1.06	
		$5d^4\ a^5D_3$	15 726.100	378.725	0.025	0.023	30.2	27.9		−1.19	−1.22	
		$5d^3(^4F)6s\ b^3F_4$	18 493.610	423.084	0.021	0.017	25.8	21.1		−1.16	−1.25	
					[0.026]	[0.016]						
421°_2	42 153.276	$5d^3(^4F)6s\ a^5F_2$	1031.416	243.106	0.066	0.091	36.0	49.6	1100^f	−1.50	−1.36	−0.02^f
	$\tau = 9.2(8)$	$5d^3(^4F)6s\ a^5F_3$	2642.302	253.018	0.120	0.030	65.4	16.4		−1.20	−1.80	
		$5d^26s^2\ a^3P_1$	5330.822	271.493	0.029	0.028	15.7	15.1		−1.76	−1.78	
		$5d^26s^2\ a^3P_2$	5657.920	273.926	0.471	0.543	256	295	2100^f	−0.54	−0.48	0.37^f
		$5d^3(^4F)6s\ b^3F_2$	9690.482	307.956	0.100	0.078	54.5	42.5		−1.11	−1.22	
		$5d^4\ a^5D_1$	13 475.416	348.601	0.018	0.026	9.85	14.1		−1.75	−1.59	
		$5d^4\ a^5D_2$	14 494.870	361.451	0.013	0.011	6.89	6.12		−1.87	−1.92	
		$5d^3(^2D2)6s\ a^3D_1$	14 627.680	363.194	0.064	0.055	34.9	30.0		−1.16	−1.23	

Table 3 – *continued*

Upper level[a]		Lower level[a]		λ (nm)[b]	BF[c]		gA (10^6 s^{-1})			log(gf)		
Assignment	E (cm^{-1}) Lifetime (ns)	Assignment	E (cm^{-1})		HFR (A)	HFR (B)	This work HFR (A)	This work HFR (B)	Previous	This work HFR (A)	This work HFR (B)	Previous
		$5d^4\ a^5D_3$	15 726.100	378.291	0.037	0.040	20.1	21.9		−1.36	−1.33	
		$5d^3(^4P)6s\ b^3P_1$	17 375.124	403.467	0.012	0.019	6.55	10.2		−1.80	−1.61	
					[0.070]	[0.079]						
444°_3	44 430.422	$5d^3(^4F)6s\ a^5F_2$	1031.416	230.349	0.255	0.256	324	326	830^f	−0.59	−0.59	-0.18^f
	$\tau = 5.5(5)$	$5d^26s^2\ a^3F_2$	3180.141	242.349	0.139	0.140	177	178	1900^f	−0.81	−0.80	0.22^f
		$5d^3(^4F)6s\ a^5F_4$	4415.750	249.833	0.087	0.061	110	78.2	1400^f	−0.99	−1.14	0.10^f
		$5d^26s^2\ a^3F_3$	6831.437	265.886	0.171	0.167	218	212	2200^f	−0.64	−0.65	0.38^f
		$5d^3(^4F)6s\ b^3F_2$	9690.482	287.769	0.124	0.130	158	166	2100^f	−0.71	−0.69	0.41^f
		$5d^26s^2\ a^3F_4$	9746.376	288.232	0.045	0.040	56.9	50.4	700^f	−1.15	−1.20	-0.06^f
		$5d^3(^2\ G)6s\ a^3G_3$	11 767.242	306.066	0.022	0.027	27.5	33.9		−1.41	−1.32	
		$5d^3(^4P)6s\ a^5P_3$	12 435.879	312.462	0.018	0.022	23.4	27.4		−1.47	−1.40	
		$5d^3(^2\ G)6s\ a^3G_4$	12 705.388	315.117	0.023	0.024	29.5	30.1		−1.36	−1.35	
		$5d^3(^4F)6s\ b^3F_3$	14 581.057	334.920	0.056	0.066	71.4	84.0	3400^f	−0.92	−0.85	0.76^f
		$5d^3(^2D2)6s\ a^3D_2$	17 168.481	366.708	0.024	0.030	30.3	37.9		−1.21	−1.12	
					[0.036]	[0.037]						
482°_2	48 223.051	$5d^3(^4F)6s\ a^5F_2$	1031.416	211.790	0.045	0.028	46.7	29.5		−1.50	−1.70	
	$\tau = 4.8(5)$	$5d^3(^4F)6s\ a^5F_3$	2642.302	219.274	0.289	0.398	301	415	1100^f	−0.66	−0.52	-0.10^f
		$5d^26s^2\ a^3F_2$	3180.141	221.892	0.117	0.049	122	50.6		−1.04	−1.43	
		$5d^26s^2\ a^3P_1$	5330.822	233.017	0.022	0.076	22.6	79.1		−1.74	−1.19	
		$5d^26s^2\ a^3F_3$	6831.437	241.463	0.035	0.031	36.4	32.3	6500^f	−1.50	−1.55	0.75^f
		$5d^3(^4F)6s\ b^3F_2$	9690.482	259.375	0.037	0.010	38.9	9.98		−1.41	−2.00	
		$5d^3(^2G)6s\ a^3G_3$	11 767.242	274.148	0.060	0.066	62.3	68.9		−1.15	−1.11	
		$5d^3(^4P)6s\ a^5P_2$	11 875.525	274.965	0.115	0.058	120	60.3	3700^f	−0.87	−1.17	0.62^f
		$5d^4\ a^5D_1$	13 475.416	287.623	0.050	0.073	52.2	76.4	4800^f	−1.19	−1.02	0.78^f
		$5d^4\ a^5D_2$	14 494.870	296.313	0.067	0.083	69.8	86.0		−1.04	−0.95	
		$5d^3(^2D2)6s\ a^3D_1$	14 627.680	297.484	0.016	0.015	16.7	16.1		−1.65	−1.67	
		$5d^4\ a^5D_3$	15 726.100	307.538	0.029	0.026	30.3	27.3		−1.37	−1.41	
		$5d^3(^2D2)6s\ a^3D_2$	17 168.481	321.817	0.018	0.011	18.6	11.4		−1.54	−1.75	
		$5d^3(^4P)6s\ b^3P_1$	17 375.124	323.973	0.046	0.043	47.9	44.6		−1.12	−1.15	
					[0.054]	[0.033]						
486°_2	48 666.557	$5d^3(^4F)6s\ a^5F_2$	1031.416	209.862	0.031	0.059	25.6	48.5		−1.77	−1.49	
	$\tau = 6.1(4)$	$5d^26s^2\ a^3F_2$	3180.141	219.777	0.042	0.076	34.4	62.6		−1.60	−1.34	
		$5d^26s^2\ a^3P_1$	5330.822	230.685	0.086	0.089	70.5	72.7		−1.25	−1.24	
		$5d^26s^2\ a^3P_2$	5657.920	232.440	0.022	0.144	18.0	118		−1.84	−1.02	
		$5d^3(^4F)6s\ b^3F_2$	9690.482	256.491	0.107	0.222	87.8	182		−1.06	−0.75	
		$5d^3(^2\ G)6s\ a^3G_3$	11 767.242	270.928	0.134	0.037	110	30.5		−0.92	−1.47	
		$5d^3(^4P)6s\ a^5P_2$	11 875.525	271.724	0.064	0.124	52.6	102		−1.23	−0.95	
		$5d^3(^4P)6s\ a^5P_3$	12 435.879	275.927	0.128	0.082	105	67.6		−0.92	−1.11	
		$5d^3(^4F)6s\ b^3F_3$	14 581.057	293.294	0.063	0.055	51.4	45.2		−1.18	−1.23	
		$5d^3(^4P)6s\ b^3P_2$	18 500.717	331.406	0.045	0.053	36.6	43.4		−1.22	−1.15	
					[0.278]	[0.059]						
487°_1	48 776.276	$5d^3(^4F)6s\ a^5F_1$	0.000	204.952	0.024	0.037	8.19	12.8		−2.29	−2.09	
	$\tau = 8.7(10)$	$5d^3(^4F)6s\ a^5F_2$	1031.416	209.380	0.047	0.021	16.1	7.10		−1.98	−2.33	
		$5d^26s^2\ a^3F_2$	3180.141	219.248	0.057	0.019	19.5	6.68		−1.85	−2.32	
		$5d^26s^2\ a^3P_2$	5657.920	231.849	0.031	0.021	10.7	7.11		−2.06	−2.24	
		$5d^3(^4F)6\ s\ b^3F_2$	9690.482	255.770	0.663	0.701	229	242	8700^f	−0.65	−0.62	0.93^f
		$5d^4\ a^5D_1$	13 475.416	283.196	0.016	0.018	5.42	6.20		−2.19	−2.13	
		$5d^3(^2D2)6s\ a^3D_1$	14 627.680	292.752	0.024	0.037	8.16	12.6		−1.98	−1.79	
		$5d^3(^2D2)6s\ a^3D_2$	17 168.481	316.286	0.025	0.036	8.69	12.3		−1.88	−1.73	
		$5d^3(^2F)6s\ c^3F_2$	22 928.648	386.773	0.027	0.028	9.21	9.80		−1.68	−1.66	
		$5d^3(^2P)6s\ c^3P_0$	23 381.348	393.668	0.016	0.020	5.44	7.05		−1.90	−1.79	
		$5d^3(^2P)6s\ a^1P_1$	23 406.021	394.050	0.010	0.016	3.62	5.46		−2.07	−1.90	
					[0.060]	[0.046]						
489°_3	48 962.626	$5d^3(^4F)6s\ a^5F_2$	1031.416	208.566	0.026	0.046	17.7	31.3		−1.94	−1.69	
	$\tau = 10.3(5)$	$5d^3(^4F)6s\ a^5F_3$	2642.302	215.820	0.015	0.020	10.2	13.5		−2.15	−2.03	
		$5d^26s^2\ a^3P_2$	5657.920	230.851	0.184	0.156	125	106	900^f	−1.00	−1.07	-0.14^f
		$5d^26s^2\ a^3F_3$	6831.437	237.282	0.092	0.047	62.6	32.0	1400^f	−1.28	−1.57	0.07^f
		$5d^3(^4F)6s\ b^3F_2$	9690.482	354.557	0.023	0.073	15.9	49.6		−1.81	−1.32	
		$5d^26s^2\ a^3F_4$	9746.376	254.919	0.035	0.050	23.7	33.9		−1.64	−1.48	
		$5d^3(^2G)6s\ a^3G_3$	11 767.242	268.771	0.017	0.020	11.3	13.6		−1.91	−1.83	

Table 3 – *continued*

Upper level[a]		Lower level[a]		λ (nm)[b]	BF[c]		*gA* ($10^6\ s^{-1}$)			log(*gf*)		
	E (cm^{-1})											
Assignment	Lifetime (ns)	Assignment	*E* (cm^{-1})		HFR (A)	HFR (B)	This work		Previous	This work		Previous
							HFR (A)	HFR (B)		HFR (A)	HFR (B)	
		$5d^3(^4P)6s\ a^5P_2$	11 875.525	269.556	0.119	0.080	80.9	54.5		−1.05	−1.23	
		$5d^3(^4P)6s\ a^5P_3$	12 435.879	273.691	0.105	0.149	71.6	101		−1.09	−0.94	
		$5d^3(^2\ G)6s\ a^3G_4$	12 705.388	275.726	0.189	0.105	129	71.4	4300[f]	−0.83	−1.09	0.69[f]
		$5d^4\ a^5D_4$	17 231.221	315.054	0.049	0.029	33.1	19.5		−1.31	−1.54	
		$5d^4\ b^3H_4$	24 432.851	407.553	0.018	0.012	12.5	8.00		−1.51	−1.70	
					[0.128]	[0.213]						
495°_2	49 592.90	$5d^3(^4F)6s\ a^5F_1$	0.000	201.577	0.023	0.020	14.5	13.1		−2.05	−2.10	
	$\tau = 7.8(3)$	$5d^3(^4F)6s\ a^5F_2$	1031.416	205.859	0.147	0.155	93.9	99.6		−1.22	−1.20	
		$5d^3(^4F)6s\ a^5F_3$	2642.302	212.923	0.272	0.326	174	209		−0.93	−0.85	
		$5d^26s^2\ a^3F_2$	3180.141	215.390	0.109	0.068	69.8	43.5		−1.31	−1.52	
		$5d^26s^2\ a^3P_1$	5330.822	225.857	0.053	0.085	33.9	54.4		−1.59	−1.38	
		$5d^26s^2\ a^3P_2$	5657.920	227.539	0.072	0.061	46.0	39.4		−1.45	−1.51	
		$5d^3(^4F)6s\ b^3F_2$	9690.482	250.536	0.017	0.019	11.2	11.9		−1.98	−1.95	
		$5d^3(^4P)6s\ a^5P_1$	10 713.345	257.128	0.011	0.026	6.82	17.0		−2.17	−1.77	
		$5d^3(^4P)6s\ a^5P_3$	12 435.879	269.048	0.024	0.028	15.6	17.9		−1.77	−1.71	
		$5d^3(^4F)6s\ b^3F_3$	14 581.057	285.534	0.041	0.024	26.3	15.1		−1.49	−1.73	
		$5d^4\ a^5D_2$	14 494.870	284.832	0.030	0.014	19.3	8.97		−1.63	−1.96	
		$5d^4\ a^5D_3$	15 726.100	295.189	0.143	0.141	91.4	90.2		−0.92	−0.93	
					[0.058]	[0.033]						
503^o_3	50 314.638	$5d^3(^4F)6s\ a^5F_2$	1031.416	202.844	0.019	0.025	27.9	36.9		−1.76	−1.64	
	$\tau = 4.8(2)$	$5d^3(^4F)6s\ a^5F_3$	2642.302	209.699	0.062	0.121	90.4	176		−1.22	−0.94	
		$5d^26s^2\ a^3F_2$	3180.141	212.092	0.296	0.272	431	397		−0.54	−0.57	
		$5d^3(^4F)6s\ a^5F_4$	4415.750	217.802	0.078	0.181	114	264		−1.09	−0.73	
		$5d^26s^2\ a^3P_2$	5657.920	223.861	0.018	0.014	26.2	19.8		−1.71	−1.83	
		$5d^3(^4F)6s\ b^3F_2$	9690.482	246.085	0.049	0.034	70.9	49.9		−1.19	−1.34	
		$5d^26s^2\ a^3F_4$	9746.376	246.424	0.046	0.023	66.5	33.8		−1.22	−1.51	
		$5d^3(^2\ G)6s\ a^3G_3$	11 767.242	259.343	0.081	0.063	118	91.3		−0.92	−1.04	
		$5d^3(^4P)6s\ a^5P_2$	11 875.525	260.074	0.022	0.012	32.7	17.0		−1.48	−1.76	
		$5d^3(^4P)6s\ a^5P_3$	12 435.879	263.922	0.034	0.029	49.0	42.7		−1.29	−1.35	
		$5d^3(^2\ G)6s\ a^3G_4$	12 705.388	265.813	0.072	0.054	105	79.4		−0.95	−1.07	
		$5d^3(^2\ G)6s\ ^3G_4$	12 966.096	267.669	0.023	0.023	33.3	33.9		−1.45	−1.44	
		$5d^3(^2H)6s\ a^3H_4$	15 851.163	290.077	0.092	0.062	134	91.0		−0.77	−0.94	
		$5d^3(^2D2)6s\ a^3D_2$	17 168.481	301.606	0.014	0.018	20.6	25.7		−1.55	−1.45	
		$5d^3(^4F)6s\ b^3F_4$	18 493.610	314.167	0.013	0.012	19.6	17.7		−1.54	−1.58	
		$5d^3(^4P)6s\ b^3P_2$	18 500.717	314.237	0.039	0.025	56.4	35.8		−1.08	−1.28	
					[0.042]	[0.032]						
521°_1	52 155.811	$5d^3(^4F)6s\ a^5F_1$	0.000	191.733	0.043	0.073	47.9	80.9		−1.58	−1.35	
	$\tau = 2.7(2)$	$5d^26s^2\ a^3F_2$	3180.141	204.117	0.029	0.076	32.8	84.3		−1.69	−1.28	
		$5d^26s^2\ a^3P_1$	5330.822	213.494	0.025	0.032	27.3	35.3		−1.73	−1.62	
		$5d^26s^2\ a^3P_2$	5657.920	214.996	0.092	0.095	102	106		−1.15	−1.14	
		$5d^3(^4P)6s\ a^5P_1$	10 713.345	241.225	0.065	0.036	72.3	39.5		−1.20	−1.46	
		$5d^26s^2\ a^3F_4$	11 875.525	248.185	0.256	0.080	284	88.4	10 000[f]	−0.58	−1.09	0.97[f]
		$5d^4\ a^5D_1$	13 475.416	258.452	0.035	0.016	38.3	17.5	13 900[f]	−1.42	−1.76	1.15[f]
		$5d^26s^2\ a^1D_2$	13 560.293	259.020	0.123	0.126	136	140	2200[f]	−0.86	−0.85	0.34[f]
		$5d^3(^2D2)6s\ a^3D_1$	14 627.680	266.388	0.167	0.265	185	294	2700[f]	−0.71	−0.50	0.46[f]
		$5d^3(^2D2)6s\ a^3D_2$	17 168.481	285.734	0.043	0.061	48.2	68.1		−1.23	−1.08	
		$5d^3(^4P)6s\ b^3P_1$	17 375.124	287.432	0.052	0.079	58.3	88.0		−1.14	−0.96	
					[0.070]	[0.061]						
525°_3	52 580.519	$5d^3(^4F)6s\ a^5F_3$	2642.302	200.182	0.082	0.075	205	187		−0.91	−0.95	
	$\tau = 2.8(2)$	$5d^3(^4F)6s\ a^5F_4$	4415.750	207.555	0.251	0.263	627	658		−0.39	−0.37	
		$5d^26s^2\ a^3P_2$	5657.920	213.050	0.114	0.098	285	246		−0.71	−0.78	
		$5d^26s^2\ a^3F_3$	6831.437	218.516	0.016	0.017	39.5	42.8		−1.55	−1.51	
		$5d^3(^4F)6\ s\ b^3F_2$	9690.482	233.082	0.040	0.046	99.4	114		−1.09	−1.03	
		$5d^26s^2\ a^3F_4$	9746.376	233.387	0.100	0.108	251	269		−0.69	−0.66	
		$5d^3(^2\ G)6s\ a^3G_3$	11 767.242	244.944	0.100	0.078	250	195		−0.65	−0.76	
		$5d^3(^4P)6s\ a^5P_2$	11 875.525	245.596	0.024	0.045	59.7	112		−1.27	−1.00	
		$5d^3(^2\ G)6s\ a^3G_4$	12 705.388	250.707	0.064	0.066	160	165		−0.82	−0.81	
		$5d^3(^2\ G)6S\ ^3G_4$	12 966.096	252.357	0.020	0.014	49.6	35.0		−1.32	−1.48	
		$5d^26s^2\ a^1D_2$	13 560.293	256.200	0.011	0.015	28.7	37.3		−1.55	−1.44	
		$5d^3(^4F)6s\ b^3F_3$	14 581.057	263.084	0.045	0.041	112	102		−0.93	−0.97	
		$5d^3(^2D2)6s\ a^3D_3$	18 553.880	293.801	0.044	0.039	110	97.1	4200[f]	−0.85	−0.90	0.74[f]

Table 3 – *continued*

Upper level[a]	E (cm^{-1})	Lower level[a]		λ (nm)[b]	BF[c]		gA (10^6 s^{-1})			log(gf)		
Assignment	Lifetime (ns)	Assignment	E (cm^{-1})		HFR (A)	HFR (B)	This work HFR (A)	This work HFR (B)	Previous	This work HFR (A)	This work HFR (B)	Previous
					[0.089]	[0.095]						
528°_{1}	52 824.611	$5d^26s^2\ a^3F_2$	3180.141	201.367	0.022	0.096	21.0	92.5		−1.89	−1.25	
	$\tau = 3.1(3)$	$5d^26s^2\ a^3P_0$	4124.858	205.274	0.082	0.061	79.1	59.2		−1.30	−1.43	
		$5d^26s^2\ a^3P_1$	5330.822	210.487	0.049	0.105	47.8	101		−1.50	−1.17	
		$5d^26s^2\ a^3P_2$	5657.920	211.947	0.034	0.033	32.5	32.4		−1.66	−1.66	
		$5d^3(^4F)6s\ b^3F_2$	9690.482	231.764	0.018	0.023	17.6	22.5		−1.85	−1.74	
		$5d^3(^4P)6s\ a^5P_1$	10 713.345	237.394	0.350	0.215	339	208	3500[f]	−0.54	−0.76	0.47[f]
		$5d^3(^4P)6s\ a^5P_2$	11 875.525	244.132	0.172	0.177	166	171		−0.83	−0.82	
		$5d^4\ a^5D_1$	13 475.416	254.059	0.064	0.074	61.8	72.0		−1.22	−1.16	
		$5d^4\ a^5D_2$	14 494.870	260.816	0.017	0.018	16.6	17.4		−1.77	−1.75	
		$5d^3(^2D2)6s\ a^3D_1$	14 627.680	261.723	0.019	0.031	17.9	29.7		−1.73	−1.52	
		$5d^3(^4P)6s\ b^3P_0$	16 288.138	273.618	0.032	0.035	31.3	33.9		−1.45	−1.42	
		$5d^3(^2D2)6s\ a^3D_2$	17 168.481	280.374	0.012	0.011	11.4	11.0		−1.87	−1.89	
		b^1D_2	23 292.812	338.544	0.012	0.018	11.6	17.0		−1.70	−1.53	
		$5d^3(^2P)6s\ c^3P_0$	23 381.348	339.539	0.018	0.022	17.4	21.7		−1.52	−1.42	
					[0.099]	[0.081]						
534°_{3}	53 465.73	$5d^26s^2\ a^3F_2$	3180.141	198.863	0.103	0.141	241	329		−0.85	−0.71	
	$\tau = 3.0(3)$	$5d^3(^4F)6s\ a^5F_4$	4415.750	203.809	0.065	0.048	152	113		−1.02	−1.15	
		$5d^26s^2\ a^3F_3$	6831.437	214.366	0.023	0.013	53.7	29.6		−1.43	−1.69	
		$5d^3(^2\ G)6s\ a^3G_3$	11 767.242	239.744	0.014	0.017	31.9	40.8		−1.56	−1.45	
		$5d^3(^4P)6s\ a^5P_2$	11 875.525	240.368	0.162	0.169	377	393	5800[f]	−0.49	−0.47	0.70[f]
		$5d^3(^4P)6s\ a^5P_3$	12 435.879	243.651	0.285	0.275	665	641	10 700[f]	−0.23	−0.24	0.98[f]
		$5d^3(^2\ G)6S\ ^3G_4$	12 966.096	246.841	0.152	0.154	355	359		−0.49	−0.48	
		$5d^3(^4F)6s\ b^3F_3$	14 581.057	257.094	0.012	0.014	27.6	33.6		−1.56	−1.48	
		$5d^3(^2H)6s\ a^3H_4$	15 851.163	265.775	0.013	0.028	29.2	66.5		−1.51	−1.15	
		$5d^4\ a^5D_4$	17 231.221	275.898	0.025	0.042	57.6	97.6		−1.18	−0.95	
		$5d^3(^2D2)6s\ a^3D_3$	18 553.880	286.352	0.018	0.016	42.3	37.4		−1.28	−1.34	
		$5d^4\ b^3H_4$	24 432.851	344.338	0.012	0.018	28.0	41.4		−1.30	−1.13	
					[0.116]	[0.065]						
536°_{2}	53 644.90	$5d^3(^4F)6s\ a^5F_2$	1031.416	190.065	0.051	0.065	91.7	117		−1.30	−1.20	
	$\tau = 2.8(2)$	$5d^3(^4F)6s\ a^5F_3$	2642.302	196.068	0.024	0.025	42.5	44.7		−1.61	−1.59	
		$5d^26s^2\ a^3P_1$	5330.822	206.913	0.049	0.063	88.2	113		−1.25	−1.14	
		$5d^26s^2\ a^3F_3$	6831.437	213.547	0.038	0.023	67.2	41.3		−1.34	−1.55	
		$5d^3(^4F)6s\ b^3F_2$	9690.482	227.438	0.103	0.094	184	167		−0.84	−0.89	
		$5d^3(^4P)6s\ a^5P_1$	10 713.345	232.858	0.016	0.016	28.5	28.4		−1.64	−1.64	
		$5d^3(^2\ G)6s\ a^3G_3$	11 767.242	238.718	0.067	0.037	120	66.7		−0.99	−1.24	
		$5d^3(^4P)6s\ a^5P_3$	12 435.879	242.591	0.127	0.061	227	109	9900[f]	−0.70	−1.02	0.94[f]
		$5d^26s^2\ a^1D_2$	13 560.293	249.397	0.079	0.079	141	141		−0.88	−0.88	
		$5d^3(^4F)6s\ b^3F_3$	14 581.057	255.951	0.014	0.015	25.5	27.5		−1.60	−1.57	
		$5d^4\ a^5D_2$	14 494.870	255.351	0.080	0.067	143	119		−0.85	−0.93	
		$5d^3(^2D2)6s\ a^3D_1$	14 627.680	256.220	0.089	0.135	160	242		−0.80	−0.62	
		$5d^3(^2D2)6s\ a^3D_2$	17 168.481	274.069	0.076	0.119	136	213	3900[f]	−0.81	−0.62	0.65[f]
		$5d^3(^4P)6s\ b^3P_2$	18 500.717	284.458	0.062	0.070	112	124		−0.87	−0.82	
		$5d^3(^2D2)6s\ a^3D_3$	18 553.880	284.889	0.056	0.066	100	118		−0.91	−0.84	
					[0.069]	[0.065]						
545°_{2}	54 533.758	$5d^26s^2\ a^3F_3$	6831.437	209.566	0.143	0.150	162	171		−0.97	−0.95	
	$\tau = 4.4(2)$	$5d^3(^4P)6s\ a^5P_1$	10 713.345	228.134	0.223	0.317	253	360		−0.70	−0.55	
		$5d^3(^2\ G)6s\ a^3G_3$	11 767.242	233.756	0.088	0.086	99.5	98.2		−1.09	−1.09	
		$5d^3(^4P)6s\ a^5P_2$	11 875.525	234.349	0.218	0.123	248	140		−0.69	−0.94	
		$5d^3(^4P)6s\ a^5P_3$	12 435.879	237.470	0.035	0.027	40.1	30.6		−1.47	−1.59	
		$5d^4\ a^5D_1$	13 475.416	243.482	0.029	0.035	32.8	39.8		−1.53	−1.45	
		$5d^26s^2\ a^1D_2$	13 560.293	243.986	0.026	0.042	30.0	47.2		−1.57	−1.38	
		$5d^3(^4F)6s\ b^3F_3$	14 581.057	250.221	0.038	0.031	42.7	34.8		−1.40	−1.49	
		$5d^4\ a^5D_3$	15 726.100	257.604	0.041	0.033	46.1	37.6		−1.34	−1.43	
		$5d^3(^4P)6s\ b^3P_1$	17 375.124	269.036	0.023	0.034	26.6	38.9		−1.54	−1.37	
		$5d^3(^2D2)6s\ b^1D_2$	23 294.812	320.021	0.019	0.011	21.7	12.4		−1.48	−1.72	
		$5d^3(^2F)6s\ c^3F_3$	23 620.395	323.392	0.029	0.028	32.5	31.8		−1.29	−1.30	
		$5d^3(^2P)6s\ ^3P_1$	26 234.671	353.267	0.011	0.012	12.2	13.9		−1.64	−1.58	
					[0.077]	[0.071]						
546°_{3}	54 648.975	$5d^26s^2\ a^3F_2$	3180.141	194.292	0.262	0.190	573	415		−0.49	−0.63	

Table 3 – *continued*

Upper level[a] Assignment	E (cm^{-1}) Lifetime (ns)	Lower level[a] Assignment	E (cm^{-1})	λ (nm)[b]	BF[c] HFR (A)	HFR (B)	*gA* (10^6 s^{-1}) This work HFR (A)	HFR (B)	Previous	log(*gf*) This work HFR (A)	HFR (B)	Previous
	$\tau = 3.2(2)$	$5d^26s^2\ a^3P_2$	5657.920	204.053	0.023	0.028	51.3	60.3		−1.49	−1.42	
		$5d^3(^4F)6s\ b^3F_2$	9690.482	222.358	0.026	0.051	56.3	112		−1.38	−1.08	
		$5d^3(^4P)6s\ a^5P_2$	11 875.525	233.718	0.113	0.040	247	87.9		−0.69	−1.14	
		$5d^3(^4P)6s\ a^5P_3$	12 435.879	236.821	0.023	0.338	49.3	739		−1.38	−0.21	
		$5d^3(^2G)6S\ ^3G_4$	12 966.096	239.834	0.061	0.117	133	257		−0.94	−0.65	
		$5d^26s^2\ a^1D_2$	13 560.293	243.302	0.076	0.013	167	27.7		−0.83	−1.61	
		$5d^3(^2F)6s\ c^3F_2$	22 928.648	315.164	0.017	0.012	37.5	25.4		−1.25	−1.42	
					[0.399]	[0.211]						
551°_3	55 128.389	$5d^26s^2\ a^3F_2$	3180.141	192.499	0.067	0.159	148	348		−1.09	−0.71	
	$\tau = 3.2(2)$	$5d^26s^2\ a^3P_2$	5657.920	202.076	0.068	0.164	150	360		−1.04	−0.66	
		$5d^26s^2\ a^3F_3$	6831.437	206.986	0.021	0.124	45.5	272		−1.53	−0.76	
		$5d^26s^2\ a^3F_4$	9746.376	220.283	0.022	0.019	48.8	40.5		−1.45	−1.53	
		$5d^3(^4P)6s\ a^5P_3$	12 435.879	234.161	0.407	0.078	891	171	6800[f]	−0.14	−0.85	0.75[f]
		$5d^3(^2\ G)6S\ ^3G_4$	12 966.096	237.107	0.113	0.019	248	42.6		−0.68	−1.44	
		$5d^4\ a^5D_3$	15 726.100	253.716	0.039	0.023	84.6	50.9		−1.09	−1.31	
		$5d^4\ a^5D_4$	17 231.221	263.793	0.098	0.012	214	26.4		−0.65	−1.56	
		$5d^3(^4P)6s\ b^3P_2$	18 500.717	272.937	0.013	0.026	28.1	57.7		−1.50	−1.19	
		$5d^3(^2D2)6\ s\ a^3D_3$	18 553.880	273.333	0.017	0.037	37.6	79.9	4600[f]	−1.38	−1.05	0.71[f]
					[0.135]	[0.339]						

[a] Assignments and *J* values are from Kramida et al. (2021) except that the one of the 50 314.638 cm^{-1} levels is from Kiess (1962), and energy values are from Windholz et al. (2016).

[b] The wavelengths below 200 nm are the vacuum values while the ones above 200 nm are the air values.

[c] Only *BF*-values greater than 0.01 are given. Values between brackets correspond to the residuals.

[d] Quinet et al. (2009)

[e] Henderson et al. (1999).

[f] Corliss & Bozman (1962).

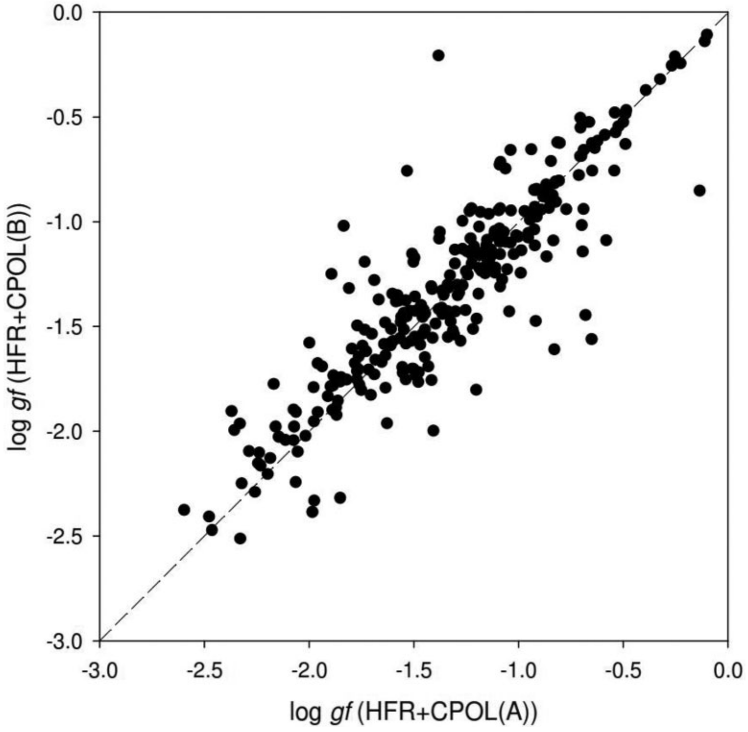

Figure 3. Comparison between the oscillator strengths (log *gf*) obtained when combining the experimental lifetimes measured in this work with branching fractions calculated using the HFR + CPOL(A) and HFR + CPOL(B) models.

as mentioned above, we can assume that the final results deduced from the latter model provide a more reliable and consistent basis for the radiative parameters listed in this work.

ACKNOWLEDGEMENTS

This work was supported by the National Natural Science Foundation of China (Grant No. U1832114). PQ is the Research Director of the Belgian F.R.S.-FNRS from which financial support is greatly acknowledged.

DATA AVAILABILITY

The data underlying this article are available in the article and in its online supplementary material.

Declaration for conflict of interest

We declare that we have no known competing financial interests or personal relationships that could have appeared to influence the work reported in this paper.

REFERENCES

Anders E., Grevesse N., 1989, Geochim. Cosmochim. Acta, 53, 197

Asplund M., Amarsi A. M., Grevesse N., 2021, A&A, 653, A141

Bergström H., Lundberg H., Persson A., Schade W., Zhao Y. Y., 1986, Phys. Scr., 33, 513

Corliss C. H., Bozman W. R., 1962, Experimental Transition Probabilities for Spectral Lines of Seventy Elements. U.S. GPO, Washington, DC, p. 407

Cowan R. D. 1981, The Theory of Atomic Structure and Spectra. California Univ. Press, Berkeley

Eriksson M., Litzén U., Wahlgren G. M., Leckrone D. S. 2002, Phys. Scr., 65, 480

Fraga S., Karwowski J., Saxena K. M., 1976, Handbook of Atomic Data. Elsevier, Amsterdam

Henderson M., Irving R. E., Matulioniene R., Curtis L. J., Ellis D. G., Wahlgren G. M., Brage T., 1999, ApJ, 520, 805

Kiess C. C., 1962, J. Res. Natl. Bur. Stand., 66A, 2

Kramida A., Ralchenko Y., Reader J., NIST ASD Team, 2021, NIST Atomic Spectra Database (ver. 5.9), National Institute of Standards and Technology, Gaithersburg, MD, https://physics.nist.gov/asd

Kwiatkowski M., Naumann F., Werner K., Zimmermann P., 1984, Phys. Lett. A, 103, 49

Langhans G., Schade W., Helbig V., 1995, Z. Phys. D, 34, 151

Moore C. E., 1958, Atomic Energy Levels, Vol. III, Natl. Bur. Stand. (US), Circ. 467. US Government Printing Office, Washington DC, p. 154

Quinet P., 2017, Can. J. Phys., 95, 790

Quinet P., Palmeri P., Biémont E., McCurdy M. M., Rieger G., Pinnington E. H., Wickliffe M. E., Lawler J. E., 1999, MNRAS, 307, 934

Quinet P., Palmeri P., Biémont E., Li Z. S., Zhang Z. G., Svanberg S., 2002, J. Alloys Compd., 344, 255

Quinet P., Fivet V., Palmeri P., Biémont É., Engström L., Lundberg H., Nilsson H., 2009, A&A, 493, 711

Schade W., Helbig V., 1986, Phys. Lett. A, 115, 39

Shang X., Wang Q., Zhang F. F., Wang C., Dai Z. W., 2015, J. Quant. Spectrosc. Radiat. Transfer, 163, 34

Siqueira M. C. et al., 2013, A&A, 550, A122

Stachowska E., Dembczyński J., Windholz J., Ruczkowski J., Elantkowska M., 2017, At. Data Nucl. Data Tables, 113, 350

Tian Y. S., Wang X. H., Yu Q., Li Y. F., Gao Y., Dai Z. W., 2016, MNRAS, 457, 1393

Wahlgren G. M., Nielsen K. E., Leckrone D. S., 2021, MNRAS, 500, 2451

Wang X. H., Quinet P., Li Q., Yu Q., Li Y. F., Wang Q., Gong Y. M., Dai Z. W., 2018, J. Quant. Spectrosc. Radiat. Transfer, 212, 112

Windholz L., Arcimowicz B., Uddin Z., 2016, J. Quant. Spectrosc. Radiat. Transfer, 176, 97

Wyart J.-F., 1977, Opt. Pura Apl., 10, 177

Wyart J.-F., Blaise J., 1990, Phys. Scr., 42, 209

This paper has been typeset from a TEX/LATEX file prepared by the author.